Carbon nanotubes as nanovectors for intracellular delivery of laronidase in Mucopolysaccharidosis type I†

T. Da Ros,*[a] A. Ostric,[a] F. Andreola,[b] M. Filocamo,[c] M. Pietrogrande,[d] F. Corsolini,[c] M. Stroppiano,[c] S. Bruni,[e] A. Serafino[b] and S. Fiorito*[b]

The immobilization of proteins on carbon nanotubes (CNTs) has been widely reported mainly for the preparation of sensors while the conjugation of enzymes for therapeutic purposes has scarcely been considered. Herein we report, to the best of our knowledge, the first example of intracellular delivery of a therapeutic enzyme by means of CNTs, retaining its activity. Mucopolysaccharidosis I is a rare genetic disease characterized by the deficiency or absence of the activity of the α-L-iduronidase (IDUA) enzyme. We evaluated the capacity of the recombinant form of the human IDUA enzyme, laronidase (Aldurazyme®), conjugated with CNTs to be internalized by fibroblasts from subjects affected with Mucopolysaccharidosis type I and the capacity of the enzyme to retain its activity after internalization. The enzyme was successfully delivered into the lysosomal space and the enzymatic activity of the conjugate was preserved after internalization up to 48 hours. This paves the way towards the use of such a kind of construct for therapeutic applications.

Accepted 24th November 2017

Introduction

Mucopolysaccharidoses (MPS) are caused by the deficiency of one of the lysosomal enzymes involved in the glycosaminoglycan (GAG) breakdown pathway.[1,2] This metabolic block leads to the accumulation of GAG in various organs and tissues of the affected patients, resulting in a multisystemic clinical picture, sometimes including cognitive impairment. Mucopolysaccharidosis type I (MPS I) is a chronic, progressive, multisystemic lysosomal storage disease characterized by the deficiency or absence of the α-L-iduronidase (IDUA) enzyme activity.[3] The progressive storage of dermatan and heparan sulfate throughout the body leads to clinical signs in various organs including short stature, dysostosis multiplex, corneal clouding, hearing loss, coarse facies, and hepatosplenomegaly, with different degrees of severity.[4] However, although the MPS I clinical phenotype represents a continuous spectrum from the severe to the attenuated forms, patients with MPS I have traditionally been classified as having three distinct phenotypes on the basis of the absence or presence and severity of CNS involvement/cognitive decline: (1) severe (Hurler syndrome, MPS IH; MIM# 607014) when the onset of symptoms is before 12 months of age, with mental retardation manifesting before the age of three and survival for no more than 10 years; (2) intermediate (Hurler/Scheie syndrome, MPS IH/S; MIM# 607015), when the onset of symptoms is between 1 and 6 years, survival is variable and mental retardation is absent or mild; and (3) 'attenuated' (Scheie syndrome, MPS IS; MIM# 607016), when symptoms first become apparent after the age of 5, survival is normal and mental retardation is never present.[1] The treatment of this disease is actually hematopoietic stem cell transplantation, while the standard medical treatment of the non-neurological manifestations is represented by the enzyme replacement therapy (ERT) performed through periodic intravenous injections.[5] ERT for MPS I is performed by intravenous administration of laronidase (Aldurazyme®, Genzyme Corporation), a protein analogous to human α-iduronidase, produced by genetic engineering in a Chinese hamster ovary cell expression system. To date, the main issues related to ERT are represented, firstly, by the fact that recombinant enzymes do not cross the blood–brain barrier and therefore are not expected to lead to any improvement in CNS damage, except if alternative routes, such as intratechal enzyme replacement therapy,[6] would be developed, and sec-

[a]INSTM unit of Trieste, Department of Chemical and Pharmaceutical Sciences, University of Trieste, Piazzale Europa 1, 34127 Trieste, Italy. E-mail: daros@units.it
[b]Institute of Translational Pharmacology, CNR, Via Fosso del Cavaliere 100, 00133 Rome, Italy. E-mail: silvana.fiorito@uniroma1.it
[c]Centro di Diagnostica Genetica e Biochimica delle Malattie Metaboliche, Istituto G. Gaslini, Via G Gaslini, 5, 16147 Genova, Italy
[d]Department of Health Sciences, Milano University, Italy
[e]Sanofi Genzyme, Italy

ondly, by the need for a weekly intravenous injection in the enzymatic treatment. Laronidase is rapidly cleared by the circulation and taken up by cellular lysosomal organelles where it is stored, but its therapeutic effectiveness does not last longer than one week.[6]

Among the emerging nanomaterials with promising applications in materials science and medicinal chemistry, carbon nanotubes (CNTs) have an important role.[7] Their discovery took place shortly after the synthesis of fullerenes in macroscopic quantities,[8] and since then the research in this exciting field has been in continuous evolution. Morphologically, CNTs consist of graphitic sheets rolled up conferring a cylindrical shape and their length is in micrometers with diameters up to 100 nm, depending on how many walls are present. Because of their extraordinary properties, CNTs can be considered attractive candidates in diverse nanotechnological applications, such as fillers in polymer matrices, molecular tanks, (bio) sensors and many others.[9] However, the lack of solubility and the difficult manipulation in solvents have imposed, until now, limitations to the use of CNTs. Indeed, the pristine CNTs in most of the organic solvents and aqueous solutions. They can be dispersed in some solvents by sonication, but precipitation occurs when this process is interrupted. There are different strategies to overcome the processing problems, and one is the formation of supramolecular complexes. CNTs can undergo chemical reactions that make them more soluble and, so far, make possible their integration into inorganic, organic and biological systems. It has been demonstrated that CNTs can interact with different classes of compounds, such as proteins and nucleic acids.[10]

Until now, enzyme immobilizations on CNTs have been mainly reported with the aim to build sensors.[11] Two different approaches can be used for the immobilization of proteins on CNTs in general: non-covalent and covalent methodologies. In the first case the conformation of the biological entity can be easily conserved but, as a drawback, there is the probable detachment of the biomolecule from the nanotubes.[12] On the other hand, the covalent functionalization establishes between the tubes and the protein a link that is stable or could be released only under specific conditions. However in the latter case, there is a possibility to hinder the catalytic site in the presence of the vector or more generally to induce a change of conformation that could lead to a decrease of the enzymatic activity.

Among the various examples reported in the literature, dihydroorotate dehydrogenase was immobilized on single walled carbon nanotubes (SWCNTs) to test the efficacy of enzyme inhibitors and an improved stability and reusability of the construct have been observed even though there was a change of K_m, probably ascribable to a partial change in the protein conformation, which however did not affect the results significantly.[13] Another example of using CNTs as a scaffold to immobilize enzymes has been proposed by Quan.[14] In this case, CNTs have been covered by acrylonitrile-based glycopolymer nanofibers and catalase has been immobilized on the mixed construct. Its performance has been compared with the native form and the one immobilized on the glycopolymer alone and it emerged that in the first case both the thermal stability and durability were significantly enhanced with respect to the other two systems. The effect of an increase of the enzymatic stability was also reported in other cases.[15] To the best of our knowledge, only one example of a direct biological use of this kind of construct has been reported for antibiotic coatings obtained by incorporating carbon nanotube–lysostaphin conjugates that are highly effective against antibiotic-resistant pathogens[16] while no publications on the therapeutic use of enzyme–CNT constructs are available. However, carbon nanostructures are investigated as vectors for the delivery of small drug molecules, oligonucleotides and antibodies.[17] These carbon nanostructures, due to their nanosized dimensions, similar to those of cell constituents, are easily internalised into the cell compartments through different ways other than receptor-mediated phagocytosis. For these reasons, they are currently under investigation as vectors for the intracellular delivery of small drug molecules, oligonucleotides and antibodies and, moreover, quite recently their capability to circumvent the blood brain barrier in animal models has been reported.[18]

We conjugated CNTs with the recombinant form of the human IDUA enzyme, laronidase, a ubiquitously expressed lysosomal glycosyl hydrolase, in order to investigate the capacity of the conjugate to be easily internalized into the cellular compartments (lysosomes), to retain the enzymatic activity even at lower doses than that usually used for the replacement therapy and to be stored for a longer time in the lysosomal compartments. To the best of our knowledge, this is the first attempt of therapeutic enzyme intracellular delivery by means of carbon nanotubes to evaluate their potential use as nanovectors for the release of enzymes in human diseases characterized by congenital enzymatic deficiency.

Experimental

Preparation of the CNT–enzyme conjugate f4-MWCNTs (Scheme 1)

Purification and oxidative cutting of CNTs. 317 mg of multiwalled carbon nanotubes (MWCNTs) 20–30 (mean diameter 25 nm, NanoAmor©) have been suspended in 200 ml of H_2SO_4/HNO_3 (3/1) solution and sonicated for 15 minutes. The suspension was left stirring under reflux at a temperature of 35–40 °C for 10 hours. Then the suspension was neutralized with 4 M NaOH, filtered and washed three times with MeOH and Et_2O. The obtained suspension was then dried and put under vacuum for one day, recovering 137 mg of oxidized nanotubes (**ox-MWCNTs**). This process was performed twice and the samples were collected together and characterized by transmission electron microscopy (TEM) and thermogravimetric (TGA) analysis (Fig. S1 and S2†, respectively). The calculated mean length of CNTs was 258 ± 100 nm, on the measurement of 97 CNTs.

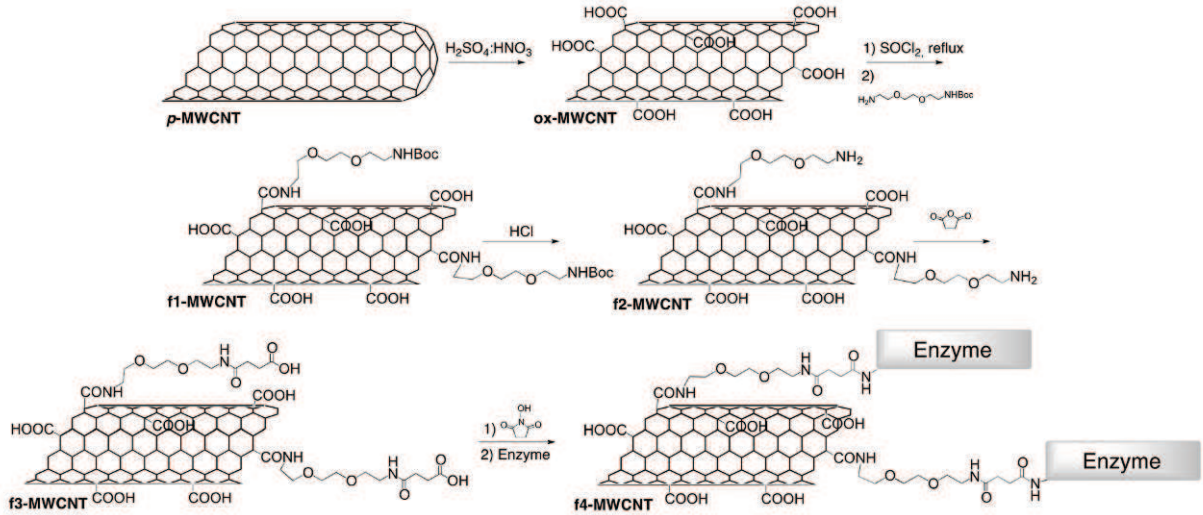

Scheme 1 Synthesis of **f4-MWCNTs**.

Preparation of f2-MWCNTs

260 mg of **ox-MWCNTs** were suspended in 20 ml of $SOCl_2$ and 0.4 ml of anhydrous DMF were added to the solution under argon to avoid the presence of water. The suspension was then sonicated at room temperature for 30 minutes under argon, and then left stirring at 75 °C for 24 hours under reflux. The product was then dried under reduced pressure and re-suspended in 80 ml of anhydrous DMF with 1.5 eq. (0.612 mmol, 85.2 μl) of triethylamine and 700 mg of *N*-Boc-diethoxy-ethyl amine. The suspension was left stirring at 90 °C under argon for 48 hours. A mixture of HCl : dioxane (1 : 4) has been added to the functionalized **f1-MWCNTs** (80 mg) and left stirring for 24 hours at r.t. The suspension has been then filtered, and washed with dioxane and ethyl acetate. Finally the suspension has been washed with methanol and Et_2O, yielding 45 mg of product **f2-MWCNTs**. From the Kaiser test, 220 μmol g^{-1} of free amino groups have been found (431 μmol g^{-1} from TGA analysis, the weight loss calculated at 450 °C).[19]

Preparation of f3-MWCNTs

22 mg of **f2-MWCNTs** (total: 4.8 μmol of free amino groups) were suspended in 10 ml of anhydrous DMF with 50 eq. of succinic anhydride (24.2 mg) and 200 μl of TEA. The suspension has been left stirring under argon pressure at r.t. overnight. Then it has been washed twice with DMF, three times with MeOH and finally with Et_2O, yielding 11.8 mg of product **f3-MWCNT**. A decrease of free amino groups was determined by the Kaiser test (58 μmol g^{-1}) and confirmed the conjugation of succinic anhydride.

Preparation of f4-MWCNTs

9 mg of **f3-MWCNTs** (degree of substitution: 153 μmol g^{-1}) have been sonicated for 20 minutes in 10 ml of anhydrous DMF. Then, under argon, a DMF solution of *N*-hydroxy-succinimide (NHS, 100 eq., 41 mg), a DMF dispersion of EDC·HCl (100 eq., 56 mg), and DIEA in excess (1 ml) have been added. After 20 minutes of sonication, the suspension was left stirring at r.t. overnight under argon. The reaction crude has been centrifuged after the addition of 10 ml of iPrOH at 4000 rpm for 5 minutes. The suspension was then washed five times with iPrOH and twice with iPrOH/Et_2O (1 : 1), then left under vacuum to remove all the solvent, yielding 7.3 mg of activated derivative, 6 mg of which were dispersed in 7 ml of sterile PBS buffer and the mixture was sonicated for 5 min. 5 mL of laronidase solution (0.58 mg mL^{-1}) was then added and the mixture was gently stirred under sterile conditions. The reaction was followed by UV-Vis, and during the reaction, suspension aliquots were taken at 0 h, after 3 h and after 96 h. Aliquots were centrifuged and the UV-Vis spectra of the supernatant were recorded: after 96 h the UV-Vis spectrum did not show traces of the enzyme in the solution. The mixture was transferred into the sterilized "Vivaspin 20" falcons with a cut-off membrane of 300 kDa. The mixture was spun 5 times at 2000 rpm for 4 min with the addition of 15 mL of fresh PBS after each spin cycle. At the last spin cycle the mixture was concentrated to 5 mL and freeze dried. Every mg of **f4-MWCNTs** corresponds to 50 U of enzyme.

Evaluation of the capacity of the conjugate f4-MWCNTs to be internalized by human fibroblasts from peripheral blood of patients affected by MPS I

Cell cultures and treatment. Dermal fibroblast cells from the skin biopsy of three unrelated patients affected with Mucopolysaccharidosis IH (MPS-1_5501, MPS-1_6806, and MPS-1_3805) were supplied by "Cell Line and DNA Biobank from patients affected by Genetic Diseases" (Istituto Gaslini, Genova, Italy). MPS-1 fibroblasts were maintained in RPMI 1640 medium (Hyclone Labs Inc., Logan, UT) supplemented with 15% (v/v) heat-inactivated fetal bovine serum (FBS) (Hyclone), L-glutamine (2 mM), penicillin (100 IU ml^{-1}) and streptomycin (100 mg ml^{-1}) and seeded on flasks and main-

tained at 37 °C in 5% CO_2. The adult human dermal primary fibroblasts HDFa, obtained from Gibco Invitrogen (Carlsbad, CA, USA), were grown in Medium 106 supplemented with the Low Serum Growth Supplement (LSGS, Invitrogen), and used as a control of normal fibroblasts. Cells were maintained at 37 °C, under a humidified atmosphere of 5% CO_2, and passaged after being detached from culture flasks with 0.05% trypsin and 0.002% EDTA solution. For *in vitro* testing, MPS-1 fibroblasts were seeded at a density of 2.5×10^4 cells per cm^2 in 35 mm culture plates or on cover-slips (∅ 10 mm), and allowed to adhere for 1–2 days before treatments. Cells were treated with the recombinant form of human α-L-iduronidase at a concentration of 5 μg ml^{-1} for 2 days, or with **f4-MWCNTs** at a laronidase concentration of 5 μg ml^{-1} and of 2.5 μg ml^{-1} for 1 and 2 days.

Ethical aspects

Following the ethical guidelines all samples for analysis and storage in Biobank were obtained with the patients' (and/or the legal guardians') written informed consent. Consent was sought using a form approved by the local Ethics Committee.

Immunocytochemical analysis

Immunocytochemical analysis was carried out on cells fixed with 4% paraformaldehyde (Sigma Aldrich) for 5 min and permeabilized with 0.2% Triton-X 100 (Sigma Aldrich) in PBS. Samples were subjected to indirect immunofluorescence staining using the specific primary mouse monoclonal antibody against human α-L-iduronidase (anti-human α-L-iduronidase/IDUA antibody – R&D System; 1 : 50 working dilution). The primary antibody was detected with the secondary AlexaFluor488-conjugated rabbit anti-mouse IgG (1 : 200 working dilution; Molecular Probes).

Samples were observed by using a LEICA TCS SP5 confocal laser scanning microscope (Leica Instruments, Heidelberg, Germany). The cell morphology was visualized by differential interference contrast (DIC), and merged images AlexaFluor488/DIC were obtained.

The quantitative analysis of the fluorescence intensity of intracellular Aldurazyme was performed under a confocal microscope by using the LasAF software (Leica Instruments). The measurement of fluorescence intensity was obtained by tracing a Region of Interest (ROI) on each cell and analyzing a minimum of 50 cells per sample. The results were given as Mean Fluorescence Intensity (MFI) per cell.

Assessment of the cell capacity to internalize the f4-MWCNT conjugate and of its capacity to localize into the lysosomal cell compartments

The uptake of the enzyme–CNT conjugate **f4-MWCNTs** was analyzed by TEM. The internalization into the lysosomal compartments was evaluated by confocal laser scanning microscopy, after double immunofluorescence staining using the mouse monoclonal antibody against human α-L-iduronidase and the rabbit polyclonal antibody against LAMP-1 (lysosomal-associated membrane protein 1; Abcam, working dilution 1 : 150).

Quantitative evaluation of the enzyme internalized into the cell

The uptake of the conjugate **f4-MWCNTs** was quantitatively evaluated by immunoblot analysis on total cell lysates.

Western blot analysis has been performed on total cell lysates from treated and untreated fibroblasts. Protein extracts were separated electrophoretically on SDS-PAGE, and proteins were electroblotted onto a PVDF membrane. The laronidase was identified using the specific antibody (anti-human α-L15 iduronidase/IDUA antibody – R&D System) and revealed with peroxidase-conjugated secondary antibodies. The blots were developed using the ECL Detection System.

Evaluation of cytotoxicity of f4-MWCNTs on fibroblast cell lines

Cell toxicity was assessed by evaluating the percentage of apoptotic/necrotic cells in the untreated control and in the samples treated with **f4-MWCNTs** and the unconjugated enzyme. For this purpose, cells were stained with propidium iodide (PI) and nuclei exhibiting the apoptotic/necrotic morphology were counted. A minimum of 200 cells per sample was analysed in a blind fashion.

Assessment of the preservation of the enzymatic activity of f4-MWCNTs after internalization

This point was evaluated through:

(a) Indirect method: Morphological evaluation of the presence of cytoplasmic inclusion bodies (CIBs), representative of glycosaminoglycan (GAG) storage in lysosomal compartments, by Transmission Electron Microscopy (TEM).

(b) Direct method: Biochemical assessment of the enzymatic activity in the cell lysates.

For the assessment of the laronidase activity, primary human normal fibroblasts (HDFa) and the treated and untreated MPS fibroblasts (MPS-1_5501, MPS-1_6806, and MPS-1_3805) were washed two times for removing the cell culture medium and detached from culture flasks with 0.05% trypsin and 0.002% EDTA solution. After washing with PBS, the cell pellet was stored at −20 °C until the biochemical assay. α-L-Iduronidase activity was assayed in the homogenates of fibroblast cell lines using 4-methylumbelliferyl-α-L-iduronide (Glycosynth, Cheshire, UK) as a substrate. Total protein was measured according to the Lowry method.

For TEM analysis, the treated and untreated fibroblasts were fixed for 2 h with 2.5% glutaraldehyde in 0.1 M Millonig's phosphate buffer (MPB) containing 2% sucrose, and then post-fixed for 8 h with 1% OsO_4 in the same buffer. Samples were then dehydrated in ascending acetone concentrations and embedded in Spurr epoxy resin (Agar Scientific Ltd, Stansted, Essex, UK). Ultrathin sections were stained with uranyl acetate and lead citrate and observed under a Philips CM12 transmission electron microscope (Philips, Eindhoven, The Netherlands) operating at 80 kV.

Results and discussion

The conjugation of CNTs with the recombinant form of the human enzyme α-L-iduronidase was successfully carried out (Scheme 1). When fibroblast cells from the skin biopsy of subjects affected with MPS IH were challenged with this compound (**f4-MWCNTs**), it was observed that the conjugate was easily internalized into the cell cytoplasm both at the enzymatic concentration of 5 μg ml^{-1}, the same used for the unconjugated enzyme, and at the enzymatic concentration of 2.5 μg ml^{-1} (Fig. 1). It is worth noting that at a lower concentration (2.5 μg ml^{-1}), the conjugate was better taken up into the cell compartments and distributed in the cytosol than the unconjugated enzyme (5 μg ml^{-1}). Moreover, in both α-L-iduronidase and **f4-MWCNT** treated samples, the laronidase derived fluorescence signal was also observed in perinuclear lysosome-like organelles (Fig. 1).

TEM performed on MPS-1_5501 fibroblasts, challenged for two days with CNT-conjugated laronidase 2.5 μg ml^{-1}, showed that nanoparticle aggregates were phagocytosed in a large quantity and internalized in cytoplasmic vacuoles (Fig. 2). Moreover, laronidase delivered by CNTs was observed to be abundantly internalized into phagolysosomes (Fig. 2 and 3), similarly to the unconjugated enzyme.

This is demonstrated by the observation that in cells treated with **f4-MWCNTs** the enzyme mainly localized in the lysosomes, as demonstrated by the tight co-localization of the laronidase–CNT conjugate with the LAMP-1 positive vesicles, compared to the cells treated with laronidase alone (Fig. 3), where, conversely, the enzyme was also observed in microvesicles dispersed in the cytosolic space.

This could be possibly due to the fact that the **f4-MWCNT** clusters are internalized by the formation of large phagosomes that directly fuse with lysosomes, as shown by TEM analysis (Fig. 2) while the free enzyme enters the cells through the endocytosis process. In fact, after binding to the mannose-6-phosphate receptors (M6PR),[20] it reaches the lysosomes after the formation of early and late endosomal vesicles.

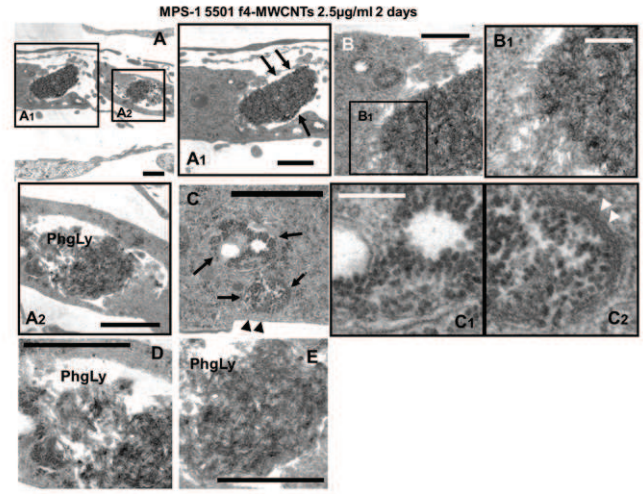

Fig. 2 Transmission electron microscopy images of MPS-1_5501 fibroblasts challenged for two days with **f4-MWCNTs** 2.5 μg ml^{-1}. Nanoparticle aggregates (arrows in A_1) were phagocytosed in a large quantity by fibroblasts (A, details in A_1 and A_2), through a tight adhesion on the cell membrane (B, detail in B_1). CNT structures were evidenced in vacuoles beneath the cell membrane (arrows in C, and details in C_1 and C_2), and in large cytoplasmic structures resembling phagolysosomes (phagLy), in (A_1, D and E). Black arrowheads in (C) point to the cell membrane, white arrowheads in C_2 point to CNTs in tight contact with the membrane of a cytoplasmic vacuole. Bars: (A), (C), D 1 μm; (B), (E) 500 nm; (E_1) 250 nm; (B_1), (B_2) 100 nm.

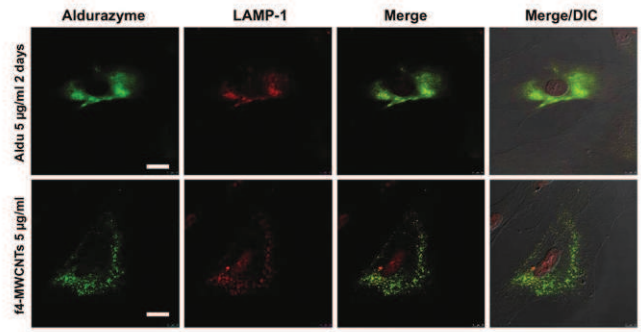

Fig. 3 Confocal microscopy images of MPS-1_5501 fibroblasts after double immunofluorescent staining of laronidase and LAMP-1. MPS-1_5501 cells were challenged for two days with laronidase 5 μg ml^{-1} and **f4-MWCNTs** 2.5 μg ml^{-1}. Green hue: laronidase; Red hue: LAMP-1; Yellow hue: co-localization sites. Merged images with cell morphology, visualized by interferential contrast (DIC) are also shown. Bars: 20 μm.

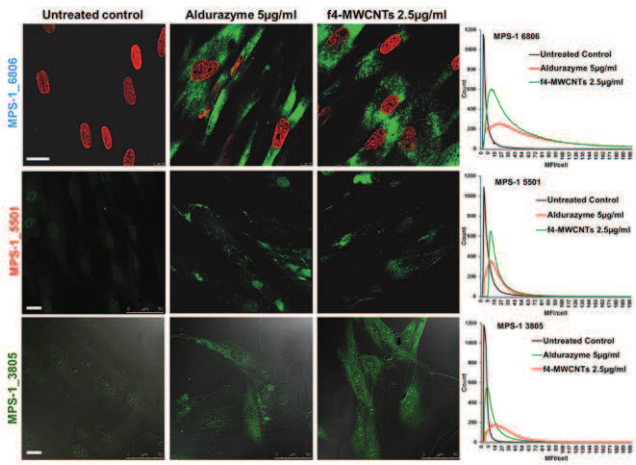

Fig. 1 Confocal microscopy images (left panels) of primary cultures of fibroblasts from three different MPS I patients (MPS-1_6806, MPS-1_5501, and MPS-1_3805) challenged for two days with laronidase 5 μg ml^{-1} or **f4-MWCNTs** 2.5 μg ml^{-1}. Three different modalities of visualization are shown: MPS-1_6806, merged images of laronidase (green hue) and nuclei staining with propidium iodide (red hue); MPS-1_5501, single immunostaining of laronidase (green hue); MPS-1_3805, merged images of laronidase (green hue) and differential interference contrast (DIC). Bars: 20 μm. Right panels: Quantitative analysis of fluorescence intensity performed using LasAF software (LEICA), as described in MM; the results are given as Mean Fluorescence Intensity (MFI) per cell, by analyzing a minimum of 50 cells per sample.

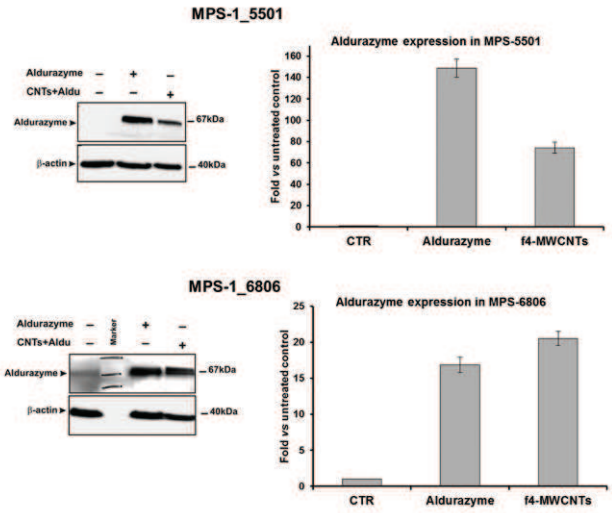

Fig. 4 Western blot analysis of laronidase expression in total cell lysates from MPS-1_5501 and MPS-1_6806 fibroblasts. Cells were challenged for two days with laronidase 5 μg ml^{-1} and **f4-MWCNTs** 2.5 μg ml^{-1}. Densitometric analysis was performed using the ImageJ processing program [http://rsbweb.nih.gov/ij/]. Values, normalized to β-actin, are reported as fold *vs.* untreated control. Data are presented as the mean ± S.D.

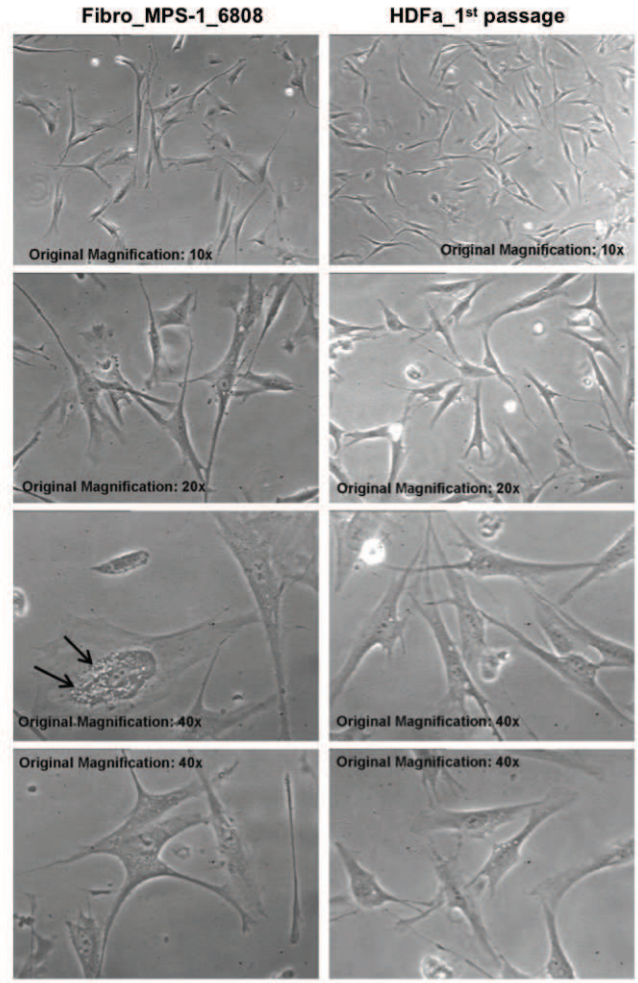

Fig. 5 Phase contrast microscopy images showing the morphology of MPS-1_6806 and HDFa control fibroblasts. Arrows point to cytoplasmic vacuolization in MPS cells.

The western blot analysis on total cell lysates from the three examined cell lines showed that laronidase was expressed at very low levels in the untreated control while its expression was significantly increased in the cells treated with both the conjugate and the unconjugated enzymes (Fig. 4).

The cytotoxicity tests showed that neither the unconjugated enzyme nor **f4-MWCNTs** were cytotoxic for the examined fibroblast cell lines, with about 2% of apoptotic and 3% of necrotic cells recorded in the untreated control as well as in the treated samples (data not shown). By optical microscopy, the morphology of the fibroblasts from patients with MPS I was very different from that of normal fibroblasts (Fig. 5). In detail, MPS-fibroblasts were larger in size and more enriched in cytoplasmic vacuoles compared to normal fibroblasts (arrows in Fig. 5).

The ultrastructural analysis of fibroblasts from patients with MPS I (MPS-1_5501 cells) showed the presence of cytoplasmic inclusion bodies (CIBs) representative of glycosaminoglycan (GAG) storage in lysosomal compartments, absent in normal fibroblasts (Fig. 6A and B). Treatment for two days with 5 μg ml^{-1} laronidase or 2.5 μg ml^{-1} **f4-MWCNTs** decreased the number and the size of CIBs (Fig. 6C and D). Moreover, in the cells treated with the CNT–enzyme conjugate, nanoparticles were observed inside GAG-containing lysosomal compartments, some of which appeared almost without GAG inclusion (Fig. 7). This indicates that CNTs delivered the enzyme in these cytoplasmic compartments, where degradation of GAGs occurs (Fig. 7C), in a similar way to that observed in the cells treated with the enzyme alone (Fig. 7B). These observations suggest that the activity of the CNT delivered enzyme is preserved inside cells, similar to that administrated alone.

The biochemical assessment of the enzymatic activity in the cell lysates confirmed that the CNT delivered laronidase preserved its activity after internalization more efficiently than the unconjugated one (Fig. 8).

Conjugated **f4-MWCNTs** (2.5 μg ml^{-1}) lead to an enzymatic activity comparable to or even higher (for the MPS-1_6806 cell line) than that obtained with a two-fold higher concentration of laronidase alone (Fig. 8). It is worth-noting that the cell line MPS-1_6806 had the higher amount of intrinsic intralysosomal laronidase (Fig. 4) and this can explain the higher level of enzymatic activity recorded in the CNT + laronidase conjugate treated cells compared to the same cell line treated with laronidase alone (Fig. 8). We can also speculate that the higher enzymatic activity observed in the MPS-1_6806 cell line and the enzymatic activity, higher than expected with a two-fold laronidase concentration, detected in the other two cell lines could be ascribed to a protective effect towards the enzymatic degradation exerted by the presence of CNTs. Indeed, the effect of

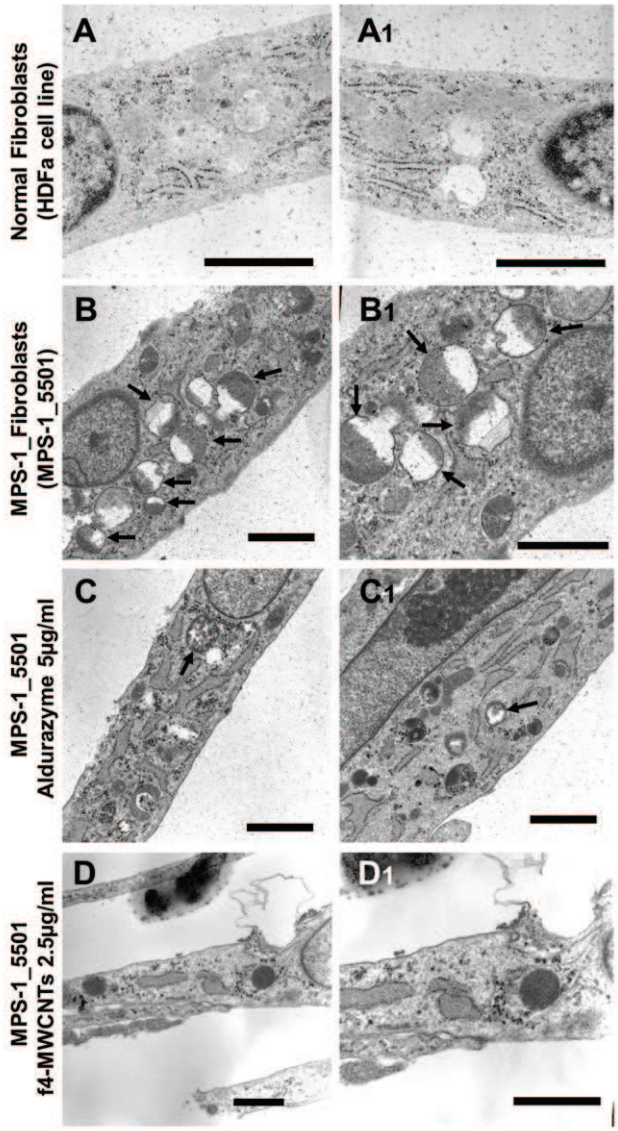

Fig. 6 Transmission electron microscopy images showing the morphology of primary human fibroblast cell line (HDFa) from control and from MPS-1_5501 challenged for two days with 5 µg ml^{-1} laronidase and **f4-MWCNTs** 2.5 µg ml^{-1}. Arrows point to cytoplasmic inclusion bodies (CIBs) representative of glycosaminoglycan (GAG) storage into lysosomal compartments. Bars 1 µm.

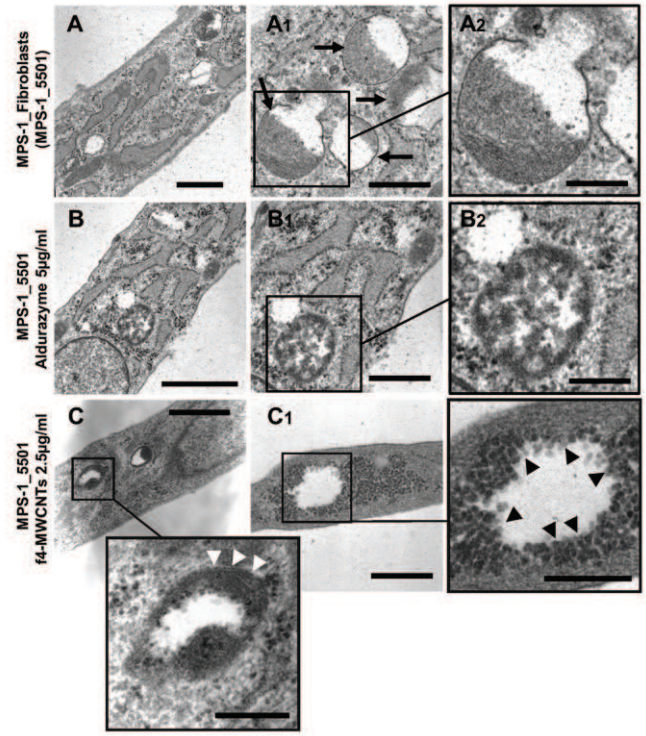

Fig. 7 Transmission electron microscopy images showing the morphology of cytoplasmic inclusion bodies (CIBs), with GAG inclusions, in MPS-1_5501 untreated fibroblasts (A) and in MPS-1_5501 fibroblasts treated for two days with the CNT–laronidase conjugate **f4-MWCNTs** (C) and the un-conjugated laronidase (B). Arrows point to CIBs; arrowheads point to CNTs inside CIBs. Bars: (A–C) 1 µm; (A_1, B_1 C_1) 500 nm; (A_2, B_2) and inset in (C, C_1) 250 nm.

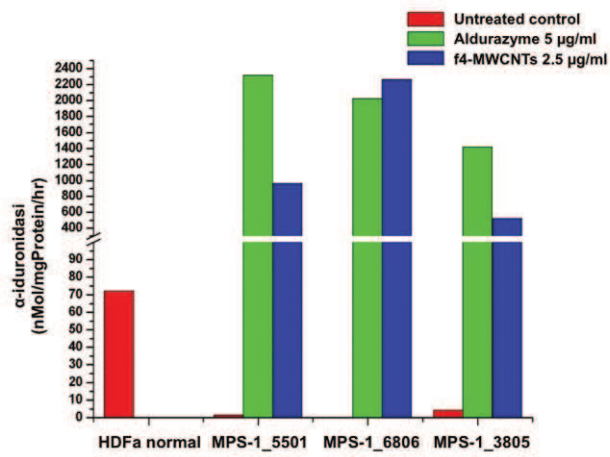

Fig. 8 Evaluation of enzymatic activity in total cell lysates from normal fibroblasts and from treated and untreated MPS fibroblasts.

an increase of the enzymatic stability was reported also in other cases.[15] Moreover, we also obtained preliminary data demonstrating that the internalized conjugate persisted inside lysosomal compartments almost up to 2 days after its removal from the culture medium.

One of the main issues related to ERT is represented by the need for a weekly intravenous injection of the enzymatic preparation. Laronidase is rapidly cleared by the circulation and taken up by cellular lysosomal organelles where it is stored, but its therapeutic effectiveness does not last longer than one week.[6] We observed that the conjugate, at an enzymatic concentration of half that of the enzyme alone, retained its activity for up to two days inside the lysosomal compartments after its removal from the culture medium. Our findings, if further studies will confirm this observation for longer periods, are very promising in order to overcome one of the main issues of ERT.

Several attempts to immobilize and/or to adsorb enzymes onto CNTs, retaining their enzymatic activity upon adsorption, have been described but in most of these studies the proteins underwent structural changes upon adsorption and the native activity was not retained or dramatically reduced.[21] Our findings show that the enzyme conjugation to MWCNTs can be successfully achieved and the resulting construct can easily be taken up into cell compartments and reach the intracellular organelles where the adsorbed enzyme can exert its activity. In addition, we demonstrated that the enzymatic activity was preserved after internalization and seemed to be even more efficient than the one exerted by the administration of the free enzyme.

Since CNTs have been considered as promising nanomaterials for biological and medical applications, intensive studies have been carried out to explore their capacity as nanovectors for the delivery of therapeutic molecules.[22]

Nevertheless, to our knowledge, the use of functionalized CNTs for intracellular enzyme delivery has not been described yet. In addition, the demonstration that the enzyme laronidase immobilized on MWCNTs was not only taken up by the lysosomes but was also able to exert the enzymatic activity more efficiently than the unconjugated one, and that its activity persisted up to 48 h allows us to foresee the potential use of the conjugate for going beyond the limits of the classical enzyme replacement therapy.

Conclusions

This is the first time that an enzyme immobilization on CNTs for biomedical applications has been successfully performed. In this study we assessed the capacity of the conjugate **f4-MWCNTs** (CNTs–laronidase) to be internalized by human fibroblasts from different patients affected with MPS I and to enter into the lysosomal space. Moreover, laronidase delivered by MWCNTs was observed to be internalized into lysosomes as well as the unconjugated laronidase, its activity was retained even at lower doses and preserved after internalization up to 48 hours. The conjugate **f4-MWCNTs** did not show any cytotoxic potential towards fibroblast cells, as well as laronidase alone. Our purpose, aimed to explore the possibility of providing a therapeutic opportunity with a more convenient cost/benefit ratio, was achieved. Thus, we believe that this construct could be exploited, upon further *in vitro* and *in vivo* investigations, for therapeutic uses.

These results pave the way for the use of carbon nanotube derivatives as drug delivery systems for the treatment of MPS and other lysosomal disorders.

Conflicts of interest

There are no conflicts to declare.

Acknowledgements

MPS I samples were obtained from the "Cell Line and DNA Biobank from patients affected by Genetic Diseases" (Istituto Giannina Gaslini), member of the Telethon Network of Genetic Biobanks (project no. GTB12001). This work was partially supported by unrestricted grants from "Cinque per mille", Ricerca Corrente, "Ministero della Salute" to MF and MS, and by a restricted grant from Sanofi Genzyme.

References

1 E. F. Neufeld and J. Muenzer, The mucopolysaccharidoses, in *The metabolic and molecular bases of inherited disease*, ed. C. R. Scriver, A. L. Beaudet, W. S. Sly and D. Valle, McGraw-Hill, New York, 7th edn, 1995, pp. 2465–2494.

2 R. Cimaz and F. La Torre, *Curr. Rheumatol. Rep.*, 2014, **16**, 389.

3 J. E. Wraith and S. Jones, *Pediatr. Endocrinol. Rev.*, 2014, **12**(Suppl 1), 102.

4 B. A. Johnson, A. Dajnoki and O. A. Bodamer, *Curr. Protoc. Hum. Genet.*, 2015, **84**, 1.

5 E. Jameson, S. Jones and T. Remmington, *Cochrane Database Syst. Rev.*, 2016, CD009354.

6 I. Nestrasil, E. Shapiro, A. Svatkova, P. Dickson, A. Chem, A. Wakumoto, A. Ahmed, E. Stehel, S. McNeil, C. Gravance and E. Maher, *Am. J. Med. Genet., Part A*, 2017, **173**, 780.

7 S. Iijima, *Nature*, 1991, **354**, 56.

8 K. Kratschmer, L. D. Lamb, K. Fostiropoulos and R. D. Huffman, *Nature*, 1990, **347**, 354.

9 N. Robertson and C. A. McGowan, *Chem. Soc. Rev.*, 2003, **32**, 96; R. H. Baughman, A. A. Zakhidov and W. A. de Heer, *Science*, 2002, **297**, 787; S. Kumar, R. Rani, N. Dilbaghi, K. Tankeshwar and K. H. Kim, *Chem. Soc. Rev.*, 2017, **46**, 158; F. Mohanty and S. K. Swain, *Curr. Org. Synth.*, 2017, **14**, 249.

10 N. Saifuddin, A. Z. Raziah and A. R. Junizah, *J. Chem.*, 2013, **2013**, 676815; S. Li, P. He, J. Dong, Z. Guo and L. Dai, *J. Am. Chem. Soc.*, 2005, **127**, 14; S. F. Oliveira, G. Bisker, N. A. Bakh, S. L. Gibbs, M. P. Landry and M. S. Strano, *Carbon*, 2015, **95**, 767.

11 To mention few examples: B. Kowalewska and K. Jakubow, *Sens. Actuators, B*, 2017, **238**, 852; K. Melzer, V. D. Bhatt, E. Jaworska, R. Mittermeier, K. Maksymiuk, A. Michalska and P. Lugli, *Biosens. Bioelectron.*, 2016, **84**, 7; X. Zhu, X. Niu, H. Zhao, J. Tang and M. Lan, *Biosens. Bioelectron.*, 2015, **67**, 79; J. V. Da Silva, D. M. Pimentel, D. E. P. Souto, R. De Cássia Silva Luz and F. S. Damos, *J. Solid State Electrochem.*, 2013, **17**, 2795; C. M. Yu, M. J. Yen and L. C. Chen, *Biosens. Bioelectron.*, 2010, **25**, 2515; Q. Chen, S. Ai, X. Zhu, H. Yin, Q. Ma and Y. Qui, *Biosens. Bioelectron.*, 2009, **24**, 2991; K. Stolarczyk, E. Nazaruk, J. Rogalski and R. Bilewicz, *Electrochim. Acta*, 2008, **53**, 3983; Q. Shi, D. Yang, Y. Su, J. Li, Z. Jiang, Y. Jiang and W. Yuan, *J. Nanopart. Res.*, 2007, **9**, 1205; S. Liu and C. Cai,

J. Electroanal. Chem., 2007, **602**, 103; J. M. Gómez, M. D. Romero and T. M. Fernández, *Catal. Lett.*, 2005, **101**, 275; J. J. Davis, K. S. Coleman, B. R. Azamian, C. B. Bagshaw and M. L. H. Green, *Chem. – Eur. J.*, 2003, **9**, 3732.

12 O. Karunwi and A. Guiseppi-Elie, *J. Nanobiotechnol.*, 2013, **11**, 6; K. Min, J. Kim, K. Park and Y. J. Yoo, *J. Mol. Catal. B: Enzym.*, 2012, **83**, 87; J. L. Felhofer, J. D. Caranto and C. D. Garcia, *Langmuir*, 2010, **26**, 17178.

13 H. Raissi and F. Mollania, *Eur. J. Pharm. Sci.*, 2014, **56**, 37.

14 J. Quan, Z. Liu, C. Branford-White, H. Nie and L. Zhu, *Colloids Surf., B*, 2014, **121**, 417.

15 P. Asuri, S. Bale, R. Pangule, D. Shah, R. Kane and J. Dordick, *Langmuir*, 2007, **23**, 12318.

16 R. Pangule, S. Brooks, C. Dinu, S. Bale, S. Salmon, G. Zhu, D. Metzger, R. Kane and J. Dordick, *ACS Nano*, 2010, **4**, 3993.

17 M. Prato, K. Kostarelos and A. Bianco, *Acc. Chem. Res.*, 2008, **41**, 60; K. Kostarelos, A. Bianco and M. Prato, *Nat. Nanotechnol.*, 2009, **4**, 627; G. Pastorin, *Pharm. Res.*, 2009, **26**, 746; K. Kostarelos, L. Lacerda, G. Pastorin, W. Wu, S. Wieckowski, J. Luangsivilay, S. Godefroy, D. Pantarotto, J. P. Briand, S. Muller, M. Prato and A. Bianco, *Nat. Nanotechnol.*, 2007, **2**, 108; R. Li, R. Wu, L. Zhao, M. Wu, L. Yang and H. Zou, *ACS Nano*, 2010, **4**, 1399; M. R. McDevitt, D. Chattopadhyay, B. J. Kappel, J. S. Jaggi, S. R. Schiffman, C. Antczak, J. T. Njardarson, R. Brentjens and D. A. Scheinberg, *J. Nucl. Med.*, 2007, **48**, 1180.

18 H. Kafa, J. Wang, N. Rubio, K. Venner, G. Anderson, E. Pach, B. Ballesteros, J. E. Preston, N. J. Abbott and K. T. Al-Jamal, *Biomaterials*, 2015, **53**, 437; J. Wang, N. Rubio, H. Kafa, E. Venturelli, C. Fabbro, C. Ménard-Moyon, T. Da Ros, J. K. Sosabowski, A. D. Lawson, M. K. Robinson, M. Prato, A. Bianco, F. Festy, J. E. Preston, K. Kostarelos and K. T. Al-Jamal, *J. Controlled Release.*, 2016, **224**, 22.

19 D. Bonifazi, C. Nacci, R. Marega, S. Campidelli, G. Ceballos, S. Modesti, M. Meneghetti and M. Prato, *Nano Lett.*, 2006, **6**, 1408; C. Annese, L. D'Accolti, V. Armuzza, T. Da Ros and C. Fusco, *Eur. J. Org. Chem.*, 2015, 3063.

20 T. Tsukimura, Y. Tajima, I. Kawashima, T. Fukushige, T. Kanzaki, T. Kanekura, M. Ikekita, K. Sugawara, T. Suzuki, T. Togawa and H. Sakuraba, *Biol. Pharm. Bull.*, 2008, **31**, 1691.

21 S. S. Karajanagi, A. A. Vertegel, R. S. Kane and J. S. Dordick, *Langmuir*, 2004, **20**, 11594; P. Zhang and D. B. Henthorn, *J. Nanosci. Nanotechnol.*, 2009, **9**, 4747; C. Caoduro, E. Hervouet, C. Girard-Thernier, T. Gharbi, H. Boulahdour, R. Delage-Mourroux and M. Pudlo, *Acta Biomater.*, 2017, **49**, 36.

22 R. Singh, D. Pantarotto, D. McCarthy, O. Chaloin, J. Hoebeke, C. D. Partidos, J. P. Briand, M. Prato, A. Bianco and K. Kostarelos, *J. Am. Chem. Soc.*, 2005, **127**, 4388; J. E. N. Dolatabadi, Y. Omidi and D. Losic, *Curr. Nanosci.*, 2011, **7**, 297; K. Bates and K. Kostarelos, *Adv. Drug Delivery Rev.*, 2013, **65**, 2023; S. K. Vashist, D. Zheng, G. Pastorin, K. Al-Rubeaan, J. H. T. Luong and F. S. Sheu, *Carbon*, 2010, **49**, 4077; W. Cheung, F. Pontoriero, O. Taratula, A. M. Chen and H. He, *Adv. Drug Delivery Rev.*, 2010, **62**, 633; L. Gao, L. Nie, T. Wang, Y. Qin, Z. Guo, D. Yang and X. Yan, *ChemBioChem*, 2006, **7**, 239; L. Lacerda, S. Raffa, M. Prato, A. Bianco and K. Kostarelos, *Nano Today*, 2007, **2**, 38.